Veterinary Microbiology 232 (2019) 1–12

Contents lists available at ScienceDirect

Veterinary Microbiology

journal homepage: www.elsevier.com/locate/vetmic

Porcine epidemic diarrhea virus infections induce apoptosis in Vero cells via a reactive oxygen species (ROS)/p53, but not p38 MAPK and SAPK/JNK signalling pathways

Xingang Xu[1], Ying Xu[1], Qi Zhang, Feng Yang, Zheng Yin, Lixiang Wang, Qinfan Li*

College of Veterinary Medicine, Northwest A&F University, Yangling, Shaanxi, 712100, China

ARTICLE INFO

Keywords:
PEDV
Apoptosis
p53 pathway
Reactive oxygen species

ABSTRACT

Porcine epidemic diarrhea virus (PEDV) is a member of Coronavirus, which causes severe watery diarrhea in piglets with high morbidity and mortality. ROS and p53 play key roles in regulating many kinds of cell process during viral infection, however, the exact function in PEDV-induced apoptosis remains unclear. In this study, the pro-apoptotic effect of PEDV was examined in Vero cells and we observed that PEDV infection increased MDM2 and CBP, promoted p53 phosphorylation at serine 20 and, promoted p53 nuclear translocation, leading to p53 activation in Vero cells. Treatment with the p53 inhibitor PFT-α could significantly inhibit PEDV-induced apoptosis. We also observed PEDV infection induced time-dependent ROS accumulation. Treatment with anti-oxidants, such as pyrrolidine dithiocarbamate (PDTC) or N-acetylcysteine (NAC), significantly inhibited PEDV-induced apoptosis.

Moreover, further inhibition tests were established to prove that p53 was regulated by ROS in PEDV-induced apoptosis. In addition, we also found that p38 MAPK and SAPK/JNK were activated in PEDV-infected Vero cells. However, treatment with the p38 MAPK inhibitor SB203580, and the SAPK/JNK inhibitor SP600125 reversed PEDV-induced apoptosis. Taken together, the results of this study demonstrate that activated p53 and accumulated ROS participated in PEDV-induced apoptosis and p53 could be regulated by ROS during PEDV infection. Activated p38 MAPK and SAPK/JNK exerted no influence on PEDV-induced apoptosis. These findings provide new insights into the function of p53 and ROS in the interaction of PEDV with Vero cells.

1. Introduction

Porcine epidemic diarrhea (PED) is a destructive infectious disease which has broken out in China and some other Asian and Western countries. It has arisen significant economic and public health concerns (Sun et al., 2016; Stevenson et al., 2013; Yang et al., 2018). PED is caused by Porcine epidemic diarrhea virus (PEDV) which is seen as an enveloped single-stranded positive-sense RNA virus belonging to the order Nidovirales, family Coronaviridae and genus Alphacoronavirus. The PEDV genome is composed of a 5′ untranslated region (5′UTR) and at least seven open reading frames (ORFs): ORF 1a/1b, spike (S), ORF3, envelope (E), membrane (M) and nucleocapsid (N), and a 3′UTR in order (Egberink et al., 1988). Consistent with pathological changes in vivo, PEDV infection could induce morphological and biochemical changes in host cells and some cell lines in vitro such as IPEC-J2 and Vero and Marc-145 (Kim and Lee, 2014; Zhao et al., 2014; Zheng et al., 2018). Previous studies have reported that PEDV induces apoptotic cell death via a mitochondrial AIF-mediated pathway (Kim and Lee, 2014) and it is S1 protein obtained from PEDV that induces apoptosis in Vero cells (Chen et al., 2018). However, little is known about the upstream signalling in PEDV-induced apoptosis. Further studies are needed to clarify which upstream signalling mechanisms are activated and involved in the regulation of apoptotic signalling pathways during PEDV infection.

The tumour-suppressor protein 53 (p53), a sequence-specific DNA binding protein, is established as transcription factor that regulates cell processes such as cell cycle arrest, senescence, apoptosis and ferroptosis (Gao et al., 2016; Laptenko and Prives, 2006). In normal conditions, p53 is stabilised at low levels by a series of regulators such as MDM2, which works as a ubiquitin ligase to help degradation of p53, whereas these processes become altered under cell stress (Kastenhuber and Lowe, 2017). In response to stimulation, p53 is activated and is

* Corresponding author.
E-mail address: liqinfan2018@163.com (Q. Li).
[1] Both authors contributed equally to this work.

https://doi.org/10.1016/j.vetmic.2019.03.028
Received 1 February 2019; Received in revised form 25 March 2019; Accepted 25 March 2019
0378-1135/

transferred into the nucleus in a phosphorylated form to regulate transcription of target genes (Bálint and Vousden, 2001). The best-understood function of p53 is its ability to promote cell cycle arrest and apoptosis (Kastenhuber and Lowe, 2017). Our previous research showed that p53 was involved in PEDV-induced Vero cell arrest, indicating that p53 may play a vital role in the mechanism of PEDV infection (Sun et al., 2018). Moreover, relying on the induction of pro-apoptotic Bcl-2 family and FasL family, p53 plays an essential role in viral infection induced apoptosis. Similar examples can be found in Canine Influenza Virus H3N2-infected MDCK cells (Zhou et al., 2017), Novel H7N9 Influenza A Virus-infected A549 cells (Yan et al., 2016) and Transmissible gastroenteritis virus-infected PK-15 cells (Huang et al., 2013). However, whether p53 participates in PEDV-induced apoptosis and the mechanism of how it impacts on apoptosis remains unclear.

Reaction oxygen species (ROS) are known toxic products in cellular metabolism. They are mainly produced by the mitochondria in most mammalian cells, act as signalling molecules, and are involved in oxidative stress during a variety of viral infections (Hamanaka and Chandel, 2010). Cells maintain a balance of ROS by means of the antioxidant system in physiological conditions (Torres et al., 2006). However, triggered by stress stimuli such as ionising radiation, chemotherapeutic drugs and viral infections, ROS can be excessively accumulated and regulate several pathological processes including proliferation, inflammation, autophagy and apoptosis (Circu and Aw, 2010; Miyata et al., 2017). Several studies showed that ROS participate in apoptosis induced by viruses. For example, parvovirus H-1 infection induces apoptosis via mediating ROS accumulation (Hristov et al., 2010). PPV infection induces ST cells apoptosis via activation of ROS generation and mitochondria-mediated apoptotic signalling (Zhao et al., 2016). ROS have also been implicated in some important apoptotic signalling pathways, such as p38 MAPK and p53 pathways (Fuh et al., 2002; Hamanaka and Chandel, 2010). For instance, during Japanese encephalitis virus (JEV) infection induced HL-CZ apoptosis, GRP78, p-ERK and p38 were activated and ROS were produced, suggesting JEV may induce apoptosis via the ERK/p38-ROS pathway (Tung et al., 2010). Treatment with 6-sho and TRAIL induced apoptosis via p53 and ROS (Nazim and Park, 2018). ROS act as important mediators that cooperate with molecular signals and participate in apoptotic signal transduction, which are consistent with the reports aforementioned. Therefore, the roles of ROS and p53 in the induction of apoptosis in PEDV-infected Vero cell lines were investigated.

In this study, we aimed to reveal whether p53 and ROS are activated during PEDV-induced apoptosis and the role that activated p53 and ROS play in the PEDV induction of apoptosis and the interrelationship between these signalling pathways. Our studies have shown that phosphorylated p53 is present in virus-infected cells and transferred to nucleus. Treatment with p53-specific inhibitors reversed PEDV-induced apoptosis both in the expression of apoptosis-related protein levels and the number of apoptotic cells, suggesting p53 plays a dominant role in PEDV-induced apoptosis. Moreover, ROS were found to be produced during this period and are closely related to apoptosis. However, activated p38 MAPK and SAPK/JNK played a limited role in PEDV-induced apoptosis. In conclusion, our findings demonstrate that p53 and ROS play significant roles in PEDV-induced apoptotic signalling pathway.

2. Materials and methods

2.1. Cells and viruses

Vero cells (ATCC, CCL-33) were grown in Dulbecco Minimal Essential Medium (DMEM; Hyclone, Logan, UT, USA) supplemented with 10% heat-inactivated foetal bovine serum (FBS; PAN-Biotech, Aidenbach, Germany), 1% penicillin/streptomycin (Invitrogen) at 37 °C in a 5% CO_2 atmosphere in an incubator. In the present study, the PEDV Shaanxi strain was isolated as previously described (Sun et al., 2018). Virus titres were determined by 50% tissue culture infective doses ($TCID_{50}$) according to the Reed and Muench method (Reed, 1938).

2.2. Inhibitors and antibodies

The p53 inhibitors PFT-α, antioxygen N-acetylcysteine (NAC) and pyrrolidine dithiocarbamate (PDTC) were purchased from Sigma. p38 MAPK inhibitor SB203580 and SAPK/JNK inhibitor SP600125 were obtained from Merk. Antibodies against p53, p-p53(Ser15), p-p53(Ser20), p-p53(Ser46), Bcl-2, Fas, p-p38 MAPK, Bax, MDM2, p300, FasL, p38 MAPK, p-SAPK/JNK, SAPK/JNK, β-actin and COX IV were purchased from Cell Signaling Technology (Danvers, MA, USA). Horseradish peroxidase (HRP)-conjugated secondary antibodies for western blot and FITC-conjugated anti-rabbit IgG were purchased from Pierce (Pierce, Rockford, IL, USA).

2.3. Apoptotic rate measurement

The Annexin V-FITC Apoptosis Kit (BioVision, Inc., CA, US) was used for apoptosis detection according to manufacturer's instructions. Briefly, cells were rinsed twice with PBS and re-suspended in 500 µl binding buffer, followed by the addition of 5 µl of Annexin V-FITC and 5 µl of PI. After incubation in the dark for 30 min at room temperature, 10,000 cells were acquired and a percentage of positive cells was analysed by flow cytometry (Becton Dickinson).

2.4. Inhibitor treatments

Pifithrin-α (PFT-α) was stored as a 10 mM stock solution in DMSO, and SB203580 and SP600125 as a 20 mM stock solution, while NAC and pyrrolidine dithiocarbamate (PDTC) were used as a 1 M and 100 mM stock solutions, respectively. PFT-α (10 µM), SB203580 (10 µM), SP600125 (10 µM), NAC (5 mM) and PDTC (50 µM) were diluted in DMEM respectively added to the culture medium, then cultivated for an hour before infection. Inhibitor was not included in the virus inoculum. After 2 h of PEDV adsorption, the virus inoculum was removed and fresh basal medium containing inhibitors was added to the culture medium. At the indicated time, the cells were collected and the related indices were detected.

2.5. Western blot analysis

Cells were harvested and rinsed with ice-cold PBS, then treated with ice-cold RIPA lysis buffer with 1 mM phenylmethyl sulphonylfluoride (PMSF). Protein concentrations were measured using BCA Protein Assay Reagent (Pierce). Equivalent amounts of proteins were loaded and electrophoresed on 8–12% sodium dodecyl sulphate-polyacrylamide gel electrophoresis (SDS-PAGE). Subsequently, proteins were transferred to polyvinylidene difluoride (PVDF) membranes (Millipore Corp, Atlanta, GA, USA). The membranes were blocked in Tris-buffered saline with 0.1% Tween 20 (TBST) containing 5% non-fat skimmed milk at room temperature for 1 h, and then incubated with indicated primary antibodies dissolved in bovine serum albumin (BSA) or non-fat milk over night at 4 °C, followed by culturation with HRP-conjugated secondary antibodies at room temperature for 1 h. The signal was detected using ECL reagent (GE Healthcare).

2.6. ROS measurement

Cells were mock-infected and PEDV-infected at different times and harvested at the same time. After rinsing three times with PBS, the cells were incubated with 10 µM DCFH-DA at 37 °C for 30 min in the dark, after rinsing three times with fresh basal medium without serum, trypsin digestion cells were used for final analysis by flow cytometry (Becton Dickinson).

2.7. Indirect immunofluorescence assay

Infected Vero samples were fixed with a mixture of cold methanol and acetone (4:1) for 20 min and blocked with 1% bovine serum albumin for 1 h. The samples were then permeabilised using Triton X-100 for 10 min and incubated for 2 h with anti-PEDV polyclonal sera (1:500) to detect PEDV and anti-p53 monoclonal antibody (1:500) to detect p53, respectively. The cells were rinsed three times for 5 min with phosphate-buffered saline (PBS) and incubated with the secondary antibody (1:50) for one hour in the dark at room temperature. Cell nuclei were counterstained with Hoechst 33258 for 5 min. After three rinses with PBS, treated cells were visually examined using a laser scanning confocal microscope (Leica Microsystems).

2.8. MTT assay

An MTT assay was carried out to determine inhibition of cell activity by inhibitors using the cell proliferation kit I (MTT) according to manufacturer's instructions (Roche Applied Science). Vero cells plated in 96-well plates, at around 90% confluence, were dosed with a corresponding concentration of inhibitor and incubated for 24 h, then 20 μl of MTT labelling reagent was added to each well and incubated at 37 °C for 4 h. After 150 μl of solubilisation solution was added, the absorbance was measured at 550 nm in an enzyme-linked immunosorbent assay reader.

2.9. Statistical analysis

All data were expressed as mean ± SD from independent experiments conducted in triplicate. Results were analysed by one-way analysis of variance (ANOVA). For each assay, Student's *t*-test were used and a value of $P < 0.05$ was considered significant.

3. Results

3.1. Cell fusion and the cytopathogenic effect produced by PEDV

PEDV infection in Vero cells generally induces typical cytopathogenic effect (CPE) such as roundup, aggregation, cell fusion, vacuolation and eventually causes cell death (Chen et al., 2018; Kusanagi et al., 1992). To determine whether apoptosis occurs in PEDV infection induced CPE and cell death, the morphological changes of PEDV-infected Vero cells were firstly observed. As shown in Fig. 1A, after PEDV was inoculated into Vero at 1 MOI for 12 h, CPE appeared in Vero cells which became more obvious at 24 h and 30 h compared to mock infection. To further reveal the propagation of PEDV in Vero cells, indirect immuno-fluorescence was carried out. Compared with 12 h post infection (h p.i.), 24 h p.i. exhibited more PEDV virion and was shown to have successfully entered the nucleus, suggesting PEDV replication occurs inside the infected cell extensively (Fig. 1B).

3.2. PEDV infection induces apoptosis in a dose-dependent manner

In order to detect the precise apoptotic rate in PEDV-infected Vero cells at MOI of 0.1, 0.5 and 1, mock and infected cells were collected at 24 h post-infection stained by Annexin V-FITC/propidium iodide(PI) (Chen et al., 2008) and analysed by flow cytometry. Representative cell apoptosis histograms and profiles in Vero cells are illustrated in Fig. 2A and B, respectively. The apoptotic rate significantly increased at different doses of PEDV infection compared with mock infection with 50.1% of apoptotic cells present at 1 MOI, suggesting PEDV induces notable apoptosis with virus post infection in a dose-dependent manner.

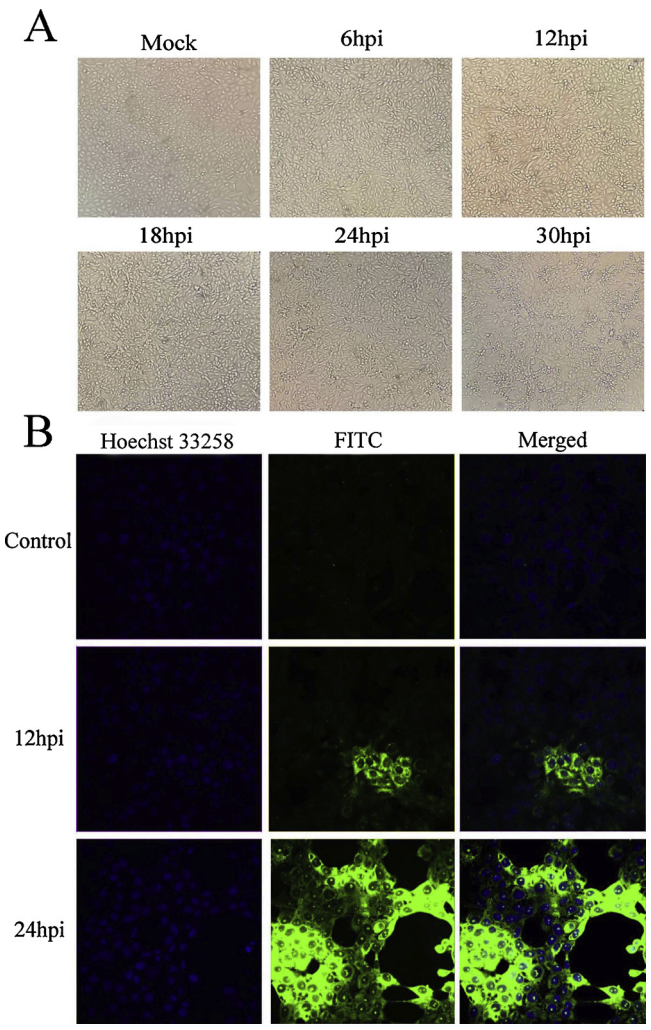

Fig. 1. Inverted microscopy and immuno-fluorescence assays of PEDV infected Vero cells. A. Cells were grown on 24-well plates and incubated with PEDV for different times, CPE appeared to start from 12 h p.i. and became more obvious at 24 h and 30 h compared with mock infection. B. Immunofluorescence assays were used to further observe intracellular propagation of PEDV in Vero cells. Vero cells were grown on coverslips in 24-well plates and infected with PEDV of 1 MOI. Cells were fixed and incubated with mouse anti-PEDV polyclonal sera (1:500) and Hoechst 33258 in mock-infected group, 12 and 24 h post infection. (fluoview 400×).

3.3. PEDV infection induces p53 signalling activation and translocation to nucleus

The tumour-suppressor protein 53 (p53) participates in multiple cell processes (Laptenko and Prives, 2006). To elucidate the mechanism of p53 in PEDV-induced apoptosis, the expressions of p53 and relative proteins were measured by western blot. From Fig. 3A and B, phosphorylated p53 at serine 20 was significantly increased at 6 h post infection compared with mock infection, and with time, p-p53(Ser20) protein level accumulated constantly, whereas p-p53(Ser15) protein levels showed no significant changes compared with the corresponding mock infection points. Interestingly, compared with mock infection, total p53 levels decreased from 18 h p.i. in PEDV infection, whereas p-p53(Ser46) protein levels showed no significant changes compared with mock infection at each time of post infection measurement and p-p53(Ser46) protein levels constantly decreased over time. Although p53 at early infection stages had no evident changes in PEDV-infected cells, its relative proteins such as p300, MDM2, CBP showed a variety of change trends in every time point of post infection(Fig. 3C and D).

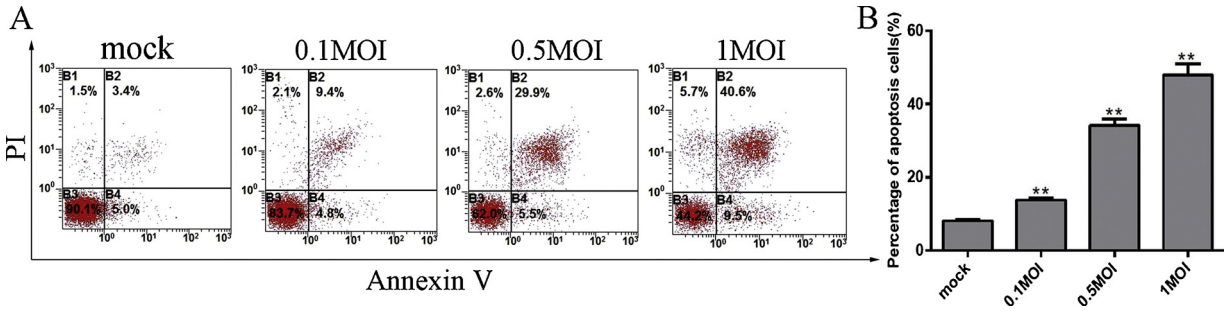

Fig. 2. PEDV infection induces apoptosis in a dose-dependent manner. A. Mock and infected Vero cells at MOI of 0.1, 0.5 and 1 were collected and stained with Annexin-V-FITC and PI at 24 h post infection, and then analysed by flow cytometry. B. Percentages of Annexin-V-FITC and PI positive cells from gated cells. Results are representative of three independent experiments. Data are represented as mean ± SD, n = 3. (*,$p < 0.05$; **, $p < 0.01$).

MDM2 increased from 6 h p.i. and continuously increased until 18 h p.i. CBP had significantly higher levels of protein at 18 h p.i. and 24 h p.i., whereas p300 increased from 0 h p.i. to 12 h p.i. and decreased from 12 h p.i. to 24 h p.i. compared with the corresponding mock infection points. These results showed that the expression of p300 increased from 6 h p.i. and peaked by 12 h p.i. and were followed by a steady decline from 12 to 24 h p.i. PEDV infection upregulated MDM2 and CBP, which might work together to cause a decrease in steady-state p53 abundance and p53 half-life in infected cells.

To further detect the subcellular localisation of p53, immunofluorescence assays were used to determine the changing position of p53 at 12 h and 24 h after PEDV infection. We observed that p53 was distributed in the whole cell including the cytoplasm and nucleus without stimulation: however, p53 progressively gathered in the nucleus upon at the stimulation of PEDV, in particular, p53 was almost exclusively found in nucleus at 24 h p.i. as shown in Fig. 3E and F. These results suggest PEDV involved in p53 nuclear translocation.

3.4. Activated p53 signalling family proteins play a vital role in PEDV induced apoptosis

To explore the relationship between p53 and apoptosis during PEDV infection, we firstly used pifithrin-a (PFT-α), a p53 specific inhibitor, to assess its inhibitory effect on p53. As shown in Fig. 4A and B, PFT-α worked well in inhibiting p-p53(Ser20), p-p53(Ser15) and p-p53(Ser46) whereas exerted limited influence on total amount of p53. Next, we investigated the relative expression of apoptotic proteins such as FasL, Bax and Bcl-2 induced by PEDV infection under PFT-α treatment. Pre-incubation of Vero cells with PFT-α in PEDV infection could evidently down-regulate Bax, upregulate Bcl-2 in protein levels, and significantly decrease the ratio of Bax/Bcl-2 in PEDV-infected Vero cells determined by Western blot assay (Fig. 4C and D). FasL protein levels were not affected by PEDV or PFT-α (Fig. 4C and E), suggesting FasL was not associated with the p53 pathway and PEDV induced apoptosis. Further inhibitor experiments should be measured by flow cytometry. Consequently, PFT-a treatment significantly decreased PEDV-induced apoptosis in Vero cells (Fig. 4F and G). These results show that p53 plays an essential role in the process of PEDV induction of cell apoptosis.

3.5. ROS were accumulated in PEDV-infected Vero cells in a time-dependent manner

ROS play an important role in the process of apoptosis and activate the mitochondria-mediated apoptotic pathway (Nazim and Park, 2018; Xu and Zhang, 2015). To investigate the role of ROS in the process of PEDV-induced apoptosis, we detected ROS level in PEDV-infected cells using DCFH-DA followed by observation under flow cytometry. The results indicate that the intensity of fluorescence was increased in PEDV-infected cells compared with control cells with mock-infection at all time-points examined, especially at 24 h post-infection (Fig. 5A). To further analyse the ROS levels, quantitative analysis of ROS in PEDV-infected cells was performed by histograms. As shown in Fig. 5B and C, ROS accumulated significantly at all the tested time points compared with control cells in a time-dependent manner ($P < 0.05$), and the relative ROS levels also increased consistently with time. All the data indicated that PEDV infection could trigger ROS accumulation in Vero cells.

3.6. Inhibition of ROS reduces PEDV-induced apoptosis

To further explore the effect of ROS on PEDV induced apoptosis in Vero cells, we used antioxidants PDTC and NAC, to suppress ROS production in PEDV infected Vero cells and evaluate the relative expression of apoptotic proteins such as Fas, FasL, Bax and Bcl-2 by Western blot. Results show that the ratio of Bax/Bcl-2 was significantly decreased compared with PEDV-infected Vero cells following NAC treatment, PDTC treatment and simultaneous treatment with both antioxidants (Fig. 6A and B). These data indicated that PDTC and NAC treatment obviously reversed PEDV-induced apoptosis, whereas the ratio of FasL/Fas showed no significant change in PEDV infection or antioxidant treatment (Fig. 6A and C). Similar results were observed by flow cytometry analysis. Both PDTC and NAC treatment significantly decreased the percentage of apoptosis in PEDV-infected Vero cells compared with those PEDV infected cells without any inhibitor treatment. When cells were treated with two antioxidants at the same time, the inhibitory effect of PEDV-induced apoptosis decreased slightly but not to any significant extent (Fig. 6D and E). These results indicated that PEDV induced apoptosis in Vero cells occurs through ROS accumulation.

3.7. Activation of p53 is partly mediated by ROS accumulation upon PEDV infection

p53 and ROS all participated in PEDV-induced apoptosis, whereas the relationship between p53 and ROS was still unclear. In this part, inhibitor experiments were carried out to clarify the relationships between two key signals. Firstly, p53 and p-p53(Ser20) were observed under the condition that cells were pre-processed with PDTC and NAC and then infected with PEDV. PDTC and NAC suppressed the expression of p53 compared with PEDV-infected cells, and treatment with the two antioxidants at same time could increase the expression level of p53. This phenomenon suggested that PEDV and antioxidants may participate in the regulation of p53 expression in a mutually antagonistic manner (Fig. 7A and B). The expression of p-p53(Ser20) significantly increased in PDTC and NAC treatment in PEDV infection compared with PEDV-infected cells without antioxidants treatment, furthermore, cells treated with two antioxidants at the same time showed a slightly decreased protein levels (Fig. 7A and C).

DCF fluorescence intensity was observed on the condition that cells were pretreated with PFT-α and then infected with PEDV. As shown in

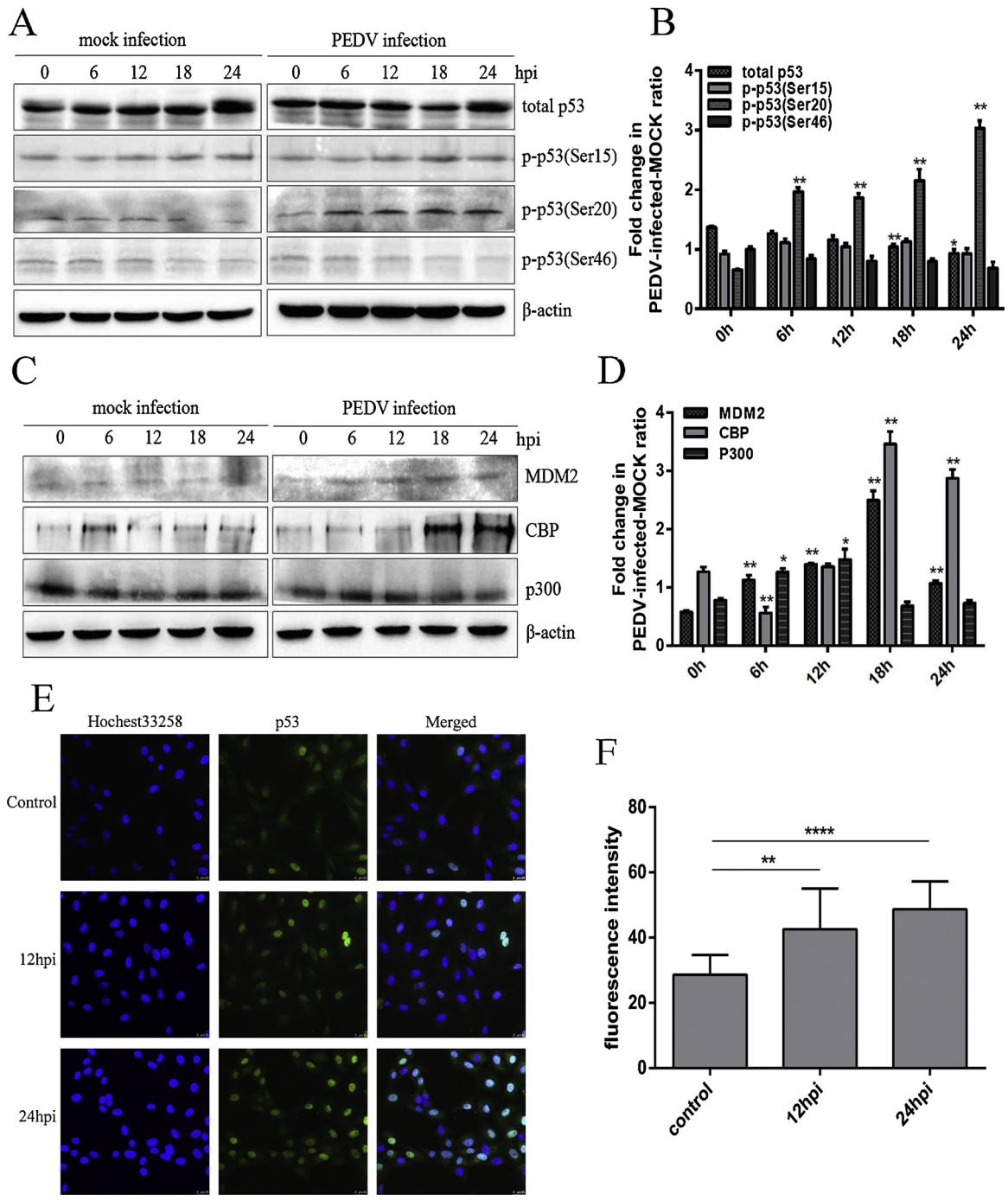

Fig. 3. PEDV infection induces p53 signalling activation and translocation to nucleus. A. Vero cells were infected with 1 MOI PEDV. Cells were collected at the indicated times and subjected to Western blot analysis using antibodies against p53 and p53-specific phosphorylation sites. B. Ratio of p-p53: total p53. Representative densitometry of p-p53 relative to total p53 was calculated after being normalised to β-actin using Image J. C. Western blot analysis of the expression of MDM2, p300 and CBP in PEDV-infected Vero cells. Vero cells were mock infected or PEDV infected for different time periods. D. Representative densitometry of MDM2, p300 and CBP was calculated after being normalised to β-actin using Image J. E. Immunofluorescence analysis of intracellular p53 protein levels. PEDV infected cells were stained with mouse anti-p53 monoclonal antibodies (1:500) and Hoechst 33258 at mock, 12 and 24 h post infection. (Fluoview 1000×) F. The levels of p53 in nucleus for each infectious period, or mock infectious period were calculated from fluorescence intensity data using Image J. Results are representative of three independent experiments. Data are represented as mean ± SD, n = 3. (*, $p < 0.05$) represents corresponding protein levels that were significantly different from those at 0 h. (**, $p < 0.01$) represents corresponding protein levels that were extremely significantly different from those at 0 h.(****, $p < 0.0001$).

Fig. 7D and E, compared to cells without PFT-α, pretreated cells generally showed higher DCF fluorescence intensity. To present the change rate of ROS more clearly, relative ROS level histograms were constructed and showed there was no significant change with PFT-α treatment (Fig. 7F), indicating ROS accumulation caused by PEDV infection was not affected by PFT-α treatment. Taken together, our data suggest that p53 is partly mediated by ROS accumulation upon PEDV infection whereas ROS production was not mediated by p53, indicating ROS was the upstream signal of p53.

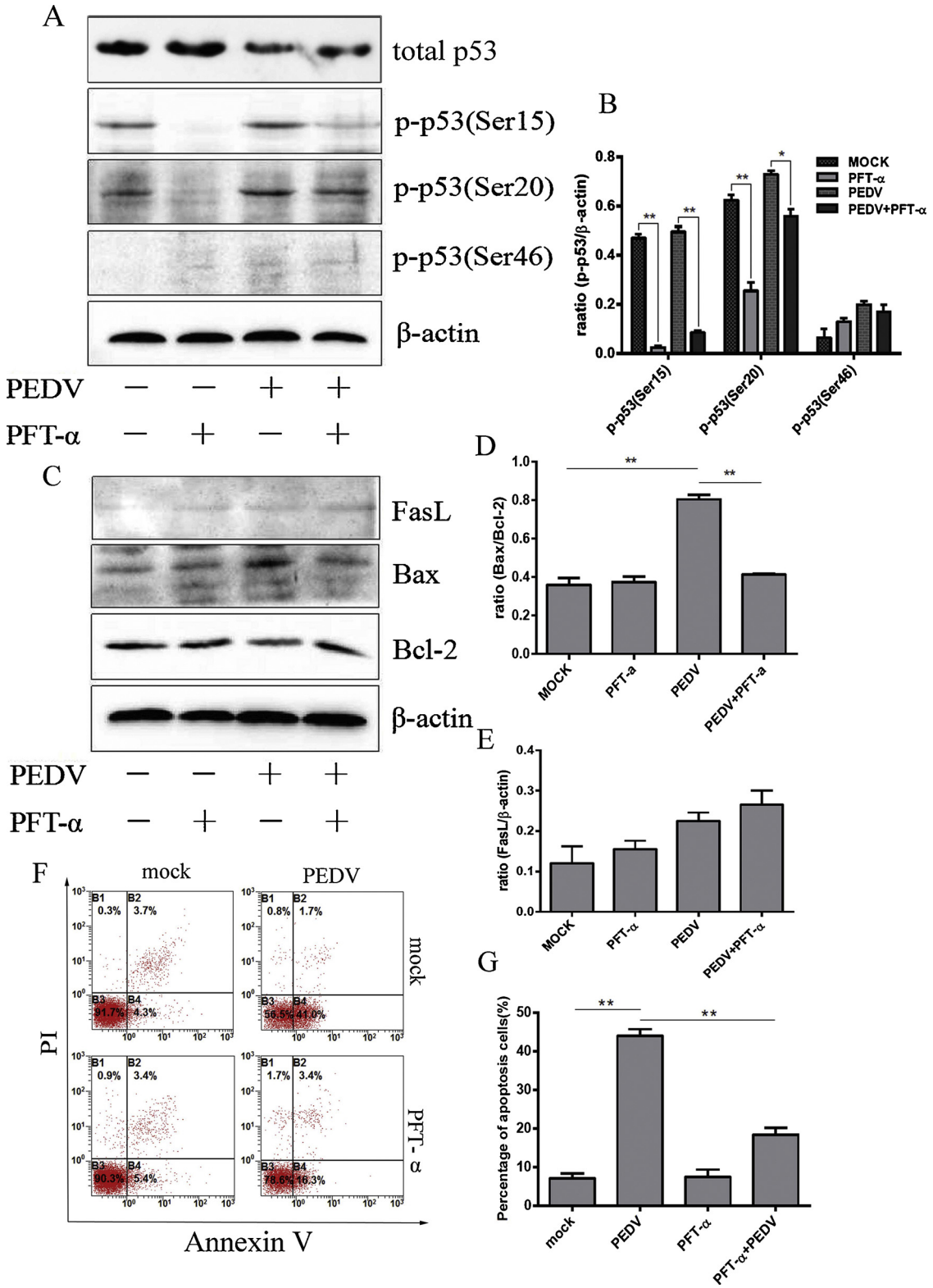

Fig. 4. Activated p53 signalling plays a vital role in PEDV induced apoptosis. A. Effect of the p53 specific inhibitor (PFT-α) on the total amount and phosphorylation of p53. Vero cells were infected with PEDV for 24 h in the presence or absence of PFT-α (10 μM). Cells were collected and subjected to Western blot analysis. B. Representative densitometry of phosphorylated p53 was calculated after being normalised to β-actin using Image J. C. Western blot analysis of the effects of PFT-α on the expression of FasL, Bcl-2 and Bax. β-actin was used as an internal control. D. The ratio of Bax/Bcl-2 was analysed in PEDV-infected Vero cells in the presence or absence of PFT-α at 24 h infection. E. Representative densitometry of FasL was calculated after being normalised to β-actin using Image J. F. Mock and infected Vero cells in the presence or absence of PFT-α were collected and stained with Annexin-V-FITC and PI at 24 h post infection, and then analysed by flow cytometry. G. Percentages of Annexin-V-FITC and PI positive cells from gated cells. Results are representative of three independent experiments. Data are represented as mean ± SD, n = 3.(*, $p < 0.05$; **, $p < 0.01$).

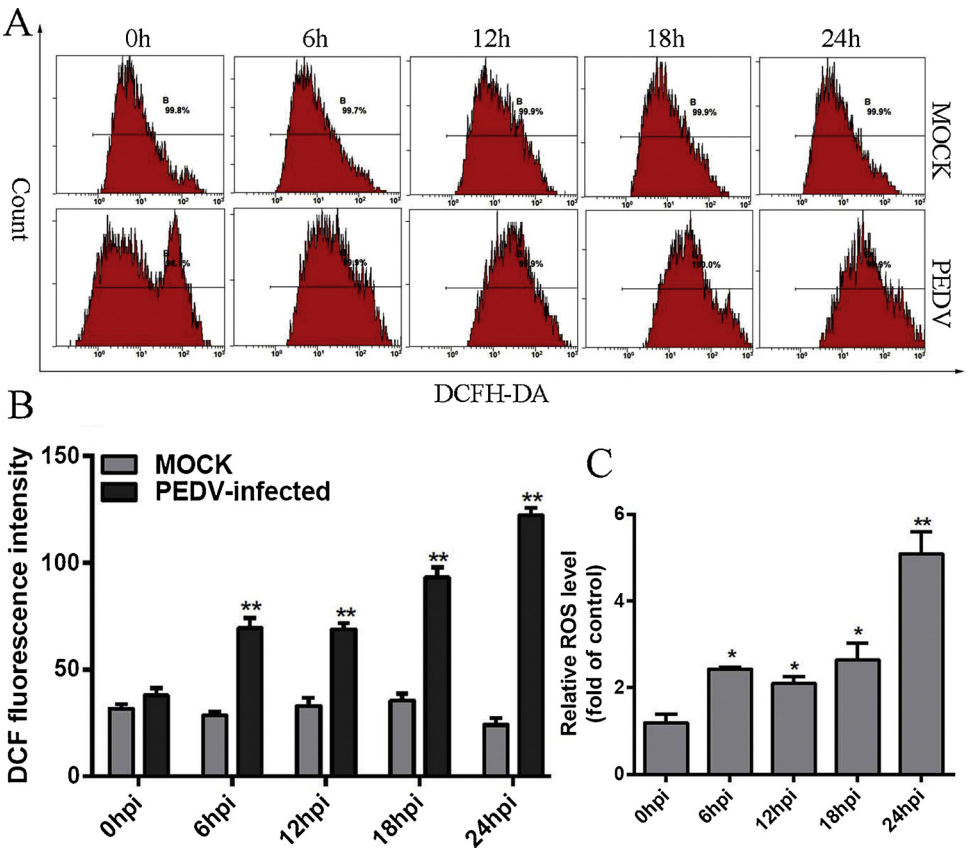

Fig. 5. ROS accumulated in PEDV-infected Vero cells via a time-dependent manner. A. Quantitative analysis of ROS in PEDV-infected Vero cells. The relative ROS levels of cells infected with PEDV at 1.0 MOI at 0, 6, 12, 18 and 24 h p.i. were analysed by flow cytometry. B. The levels of ROS for each infectious time or mock infectious time were calculated by the DCF fluorescence intensity in PEDV-infected cells. C. The relative ROS levels were calculated by the DCF fluorescence intensity in PEDV-infected cells. Results are representative of three independent experiments. Data are represented as mean ± SD, n = 3. (*, $p < 0.05$; **, $p < 0.01$).

3.8. MAPK signalling was activated in PEDV-infection which was not related to PEDV-induced apoptosis

The MAPK pathway is mainly divided into three components including the p38 MAPK, JNK and ERK pathways, and plays an important role in a variety of events in cell processes (Gary and Johnson, 2002; Xu and Zhang, 2015). Increasing evidence has shown that activated p38 MAPK and SAPK/JNK participated in regulation of p53 and ROS-mediated apoptosis (Dabiri et al., 2018; Lan et al., 2017; Shang et al., 2017). Therefore, we determined the effect of PEDV infection on the p38 MAPK and SAPK/JNK signal pathways in Vero cells. The results showed that phospho-p38 MAPK and phospho-SAPK/JNK were triggered by PEDV infection. Compared with mock infection, the protein expression remained at a high level after PEDV infection (Fig. 8A and B), indicating p38 MAPK and SAPK/JNK can be activated during PEDV infection. Next, the specific inhibitors SB203580 and SP600125 were used to block the expression of p38 MAPK and SAPK/JNK, to observe whether p38 MAPK and SAPK/JNK were involved in PEDV-induced apoptosis. As shown in Fig. 8C–E, the inhibitors worked well in our system. The ratio of Bax/Bcl-2, however, exhibited had little change following inhibitor treatment compared with the non-treated PEDV-infected cells, suggesting suppression of p38 MAPK and SAPK/JNK was unable to prevent apoptosis caused by PEDV infection (Fig. 8C and F). Our data indicated that the p38 MAPK and SAPK/JNK signalling pathways are not linked to PEDV-mediated apoptosis.

3.9. Molecular inhibitors had no inhibitory effect on cells activity

To exclude the effect of inhibitors on the toxicity of cells, we tested the inhibitory effect of cells in the presence of inhibitor and antioxidant treatment for 24 h. Cell proliferation analysis was performed by MTT assay and showed that there was no significant influence under cells treated with inhibitor and antioxidant for 24 h (Fig. 9).

4. Discussion

PEDV, an Alphacoronavirus that causes severe intestinal diarrhea in piglets, has posed a major threat to the swine industry in China since 2010. Extensive outbreaks have occurred in the United States since 2013, and have caused significant economic costs to livestock breeding (Stevenson et al., 2013; Sun et al., 2016). However, the pathogenesis of PEDV has not yet been fully clarified and further research is needed. Apoptosis, a programmed cell death process that occurs in a variety of differentiated cells, is to protect organism from damage induced by stimulation (Elmore, 2007). It is important to note that the relationship between viral infection and cell apoptosis is bidirectional. In response to viral infections, induction of apoptosis in infected cells can prevent viral replication, dissemination or persistent viral infection of the cell to protect organisms from further damage. During infection by some virues, host cells acquire resistance to apoptosis and survive for a long time which benefits viral replication. Important findings have indicated that PEDV induces apoptotic cell death via the mitochondrial AIF-mediated pathway (Kim and Lee, 2014) and it is the S1 protein obtained from PEDV that induces apoptosis in Vero cells (Chen et al., 2018). However, little is known about the changes of upstream signals such as ROS and p53 in PEDV-induced apoptosis. Also, it is unclear whether these signalling changes are caused by the direct or indirect effects of apoptosis and how these signals are regulated remains to be confirmed in Vero cells. In this study, we firstly demonstrated that PEDV infection induced apoptosis in Vero cells via activation of the p53-mediated pathway and that PEDV-induced intracellular ROS accumulation was involved in promoting apoptosis.

Regulation of cell apoptosis involves the activation of many cell signalling pathways (Barber, 2001). p53 signalling is involved in different essential cellular events and functions, such as the cell cycle, cell differentiation, apoptosis and inflammation in specific cell types upon different stresses (Laptenko and Prives, 2006). In coronaviruses, we previously found that PEDV, through the p53-dependent pathway,

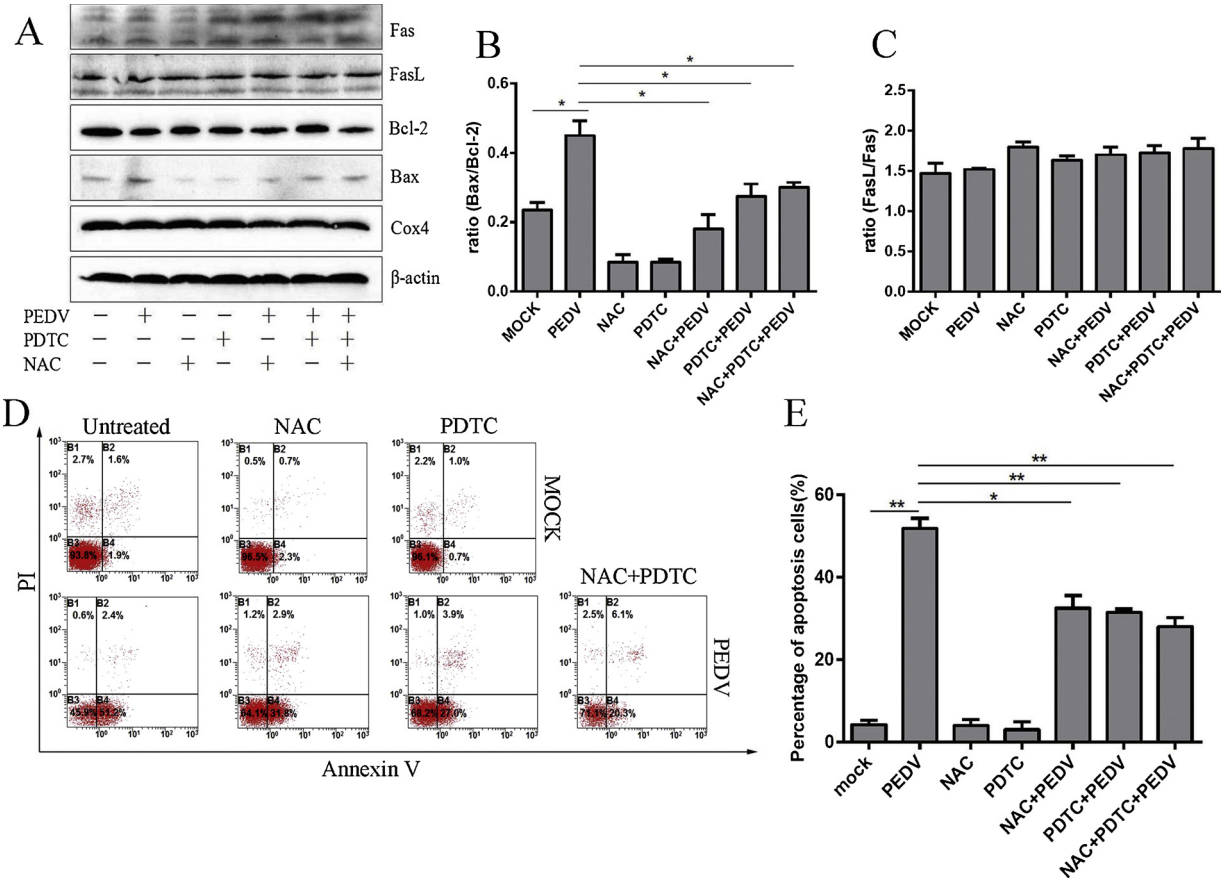

Fig. 6. Inhibition of ROS reduced PEDV-induced apoptosis. A. Western blot analysis of Fas, FasL, Bcl-2 and Bax levels in PEDV infected Vero cells in the presence or absence of antioxidant at 24 h post-infection. β-actin and Cox4 were used as internal controls. B. The ratio of Bax/Bcl-2 was analysed in PEDV-infected Vero in the presence or absence of antioxidant after 24 h infection. C. The ratio of FasL/Fas was analysed in PEDV-infected Vero cells in the presence or absence of antioxidant after 24 h infection. D. Mock and infected Vero cells in the presence or absence of antioxidant were collected and stained with Annexin-V-FITC and PI at 24 h post infection, and analysed by flow cytometry. E. Percentages of Annexin-V-FITC and PI positive cells from gated cells. Results are representative of three independent experiments. Data are represented as mean ± SD, n = 3. (*, $p < 0.05$; **, $p < 0.01$).

causes cell cycle arrest in the G0/G1 phase in Vero cells (Sun et al., 2018), which was similar to the behaviour observed with MHV in mouse fibroblast 17Cl-1 cells (Chen et al., 2004). Porcine parvovirus infection induces apoptosis in PK-15 cells through activation of p53 and mitochondria-mediated pathway (Zhang et al., 2015) SARS-CoV 3a protein causes p38 MAPK-mediated upregulation of p53, which plays an important role in 3a protein-mediated apoptosis (Mizutani et al., 2004). In the present study, PEDV infection promoted expression of p53 phosphorylation at serine 20 from 6 h p.i. to 24 h p.i. at a high level, which was similar to the trends of MDM2, whilst CBP accumulated from 18 h p.i. to 24 h p.i., indicating phosphorylated p53 was triggered under PEDV infection. The expression of total p53 was steady before 12 h p.i. and declined slightly from 18 h p.i. to 24 h p.i.. Similarly, indirect immunofluorescence assay results showed p53 gathered in the nucleus gradually whilst the fluorescence intensity changed little with prolonged infection time. The expression of p300 increased from 6 h p.i. and peaked at 12 h p.i. This was followed by a steady decline from 12 to 24 h p.i., which may be due to the different roles and effects of virus and host cells at different regulation patterns in the p53 signalling pathway. These data suggest that p53 and relative protein regulation is a complex process in virus-infected cells. Bcl-2 family members are known to be important gatekeepers of apoptotic responses (Bao, 1996; Carpio et al., 2015; Tang and Wu, 2016). Bcl-2 family members are classified into the following three functional groups: Anti-apoptotic factors such as Bcl-2, pro-apoptotic factors such as Bax, and pro-apoptotic activators, such as NOXA and PUMA (Carpio et al., 2015; Gallenne et al., 2009). Bcl-2 binds and interacts with Bax to prevent mitochondrial pore formation, which subsequently inhibits the execution of cell apoptosis. Therefore, the Bax/Bcl-2 ratio may be used to determine apoptosis (Cory et al., 2003). Here, we observed a significantly decreased ratio of Bax/Bcl-2 in PEDV infected cells and PFT-α was able to reverse the high expression of Bax/Bcl-2. These data suggested the inhibition of p53 could markedly reverse PEDV-induced apoptosis, which has the same results as the inhibition experiments confirmed by flow cytometry.

ROS are secondary products of aerobic metabolic events that mainly include oxygen free radicals such as superoxide O_2-, OH-radicals, HO_2- and some non-radical substances such as peroxide H_2O_2 and HNOO- (Hamanaka and Chandel, 2010). In the present study, PEDV disturbed the homeostatic balance between the generation and elimination of ROS, leading to the accumulation of ROS at every corresponding time after infection. Accumulating evidence from some studies has revealed that ROS are related to apoptosis in many viral infections (Hristov et al., 2010; Zhao et al., 2016; Tung et al., 2010). Since ROS were accumulated during PEDV infection, further studies should be undertaken to determine whether ROS are related to apoptosis. Therefore, antioxidant treatment of PDTC and NAC was used to test this hypothesis. We found that antioxidants were able to protect cells from PEDV-induced apoptosis regardless of the expression of apoptotic proteins or the number of apoptotic cells, suggesting that ROS plays an important role in the process of PEDV induction in cell apoptosis. However, as the application of antioxidants at the concentrations used in our experiments did not completely protect the cells from apoptosis, it appears that PEDV-induced apoptosis in infected cells may involve other uncharacterised

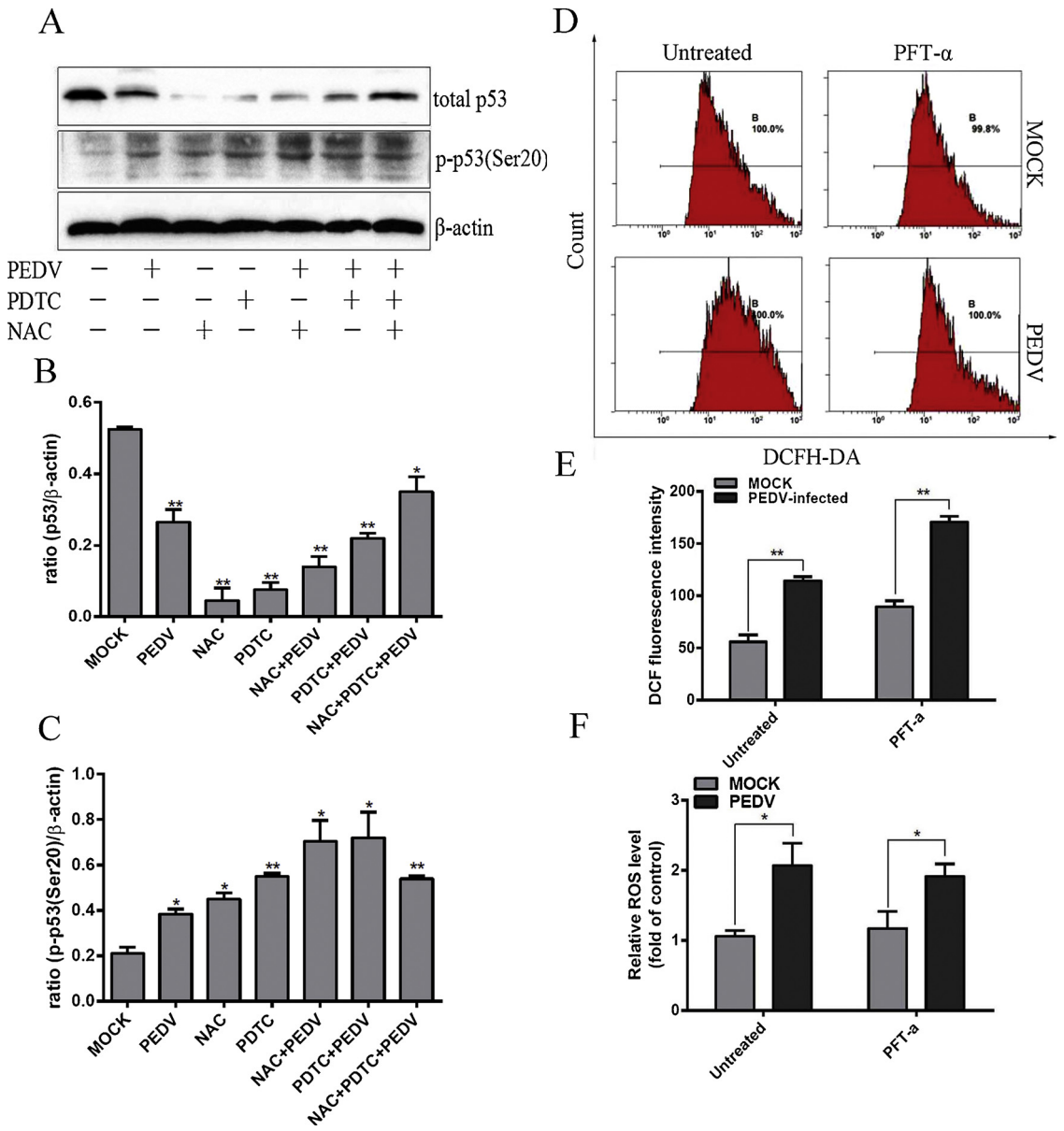

Fig. 7. Activation of p53 is partly mediated by ROS accumulation upon PEDV infection. A. Western blot analysis of p53 and phosphorylated p53 levels in PEDV infected Vero cells in the presence or absence of antioxidant at 24 h post-infection. β-actin was used as an internal control. B. The ratio of p53/β-actin was analysed and presented as a histogram. C. The ratio of phosphorylated p53/β-actin was analysed and presented as a histogram. D. Mock and infected Vero cells in the presence or absence of PFT-α were collected and stained with Annexin-V-FITC and PI at 24 h post infection, and then analysed by flow cytometry. E. The levels of ROS in the presence or absence of PFT-α were calculated by the DCF fluorescence intensity in PEDV-infected cells. F. The relative ROS level was calculated by the DCF fluorescence intensity in PEDV-infected cells. Results are representative of three independent experiments. Data are represented as mean ± SD, n = 3. (*,$p < 0.05$; **, $p < 0.01$).

mechanisms acting in parallel with ROS.

In mammalian cells, ROS serve as second messengers that mediate diverse redox-sensitive signalling pathways such as the MAPK and p53 signalling pathways (Bragado et al., 2007). Accumulating evidence supports the notion that either ROS accumulation, the p53 pathway or both may play critical roles in viral-induced apoptosis. Our study has shown that ROS and p53 all participate in PEDV-induced apoptosis, yet their relationships need to be further investigated. In this study, Western blot assays revealed inhibition of ROS could reduce p53 expression whereas treated with two antioxidants at same time and then infected with PEDV, p53 increased indicating PEDV and antioxidants may participate in the regulation of p53 expression in a mutually antagonistic manner. Moreover, results from the DCFH-DA assay suggested that PFT-α cannot reverse ROS accumulation induced by PEDV infection. MAPKs are a family of serine/threonine kinases that produce intracellular signals in response to various stimuli (Hao et al., 2015). The oxidative stress-dependent activation of MAPKs was found to be involved in the induction of cell apoptosis. Here, we also observed that phospho-p38 MAPK and phospho-SAPK/JNK were triggered by PEDV infection and that protein expression remained at a high level after PEDV infection (Fig. 8A and B), indicating p38 MAPK and SAPK/JNK can be activated during PEDV infection. However, the ratio of Bax/Bcl-2 showed little change following inhibitor treatment, in agreement with previous studies (Lee et al., 2016). Taken together, these results clearly indicate that the PEDV dependent ROS/p53 mediated pathway induced apoptosis in Vero cells whereas p38 MAPK and SAPK/JNK were not involved in apoptosis.

Molecular inhibitors were used to inhibit signalling pathways

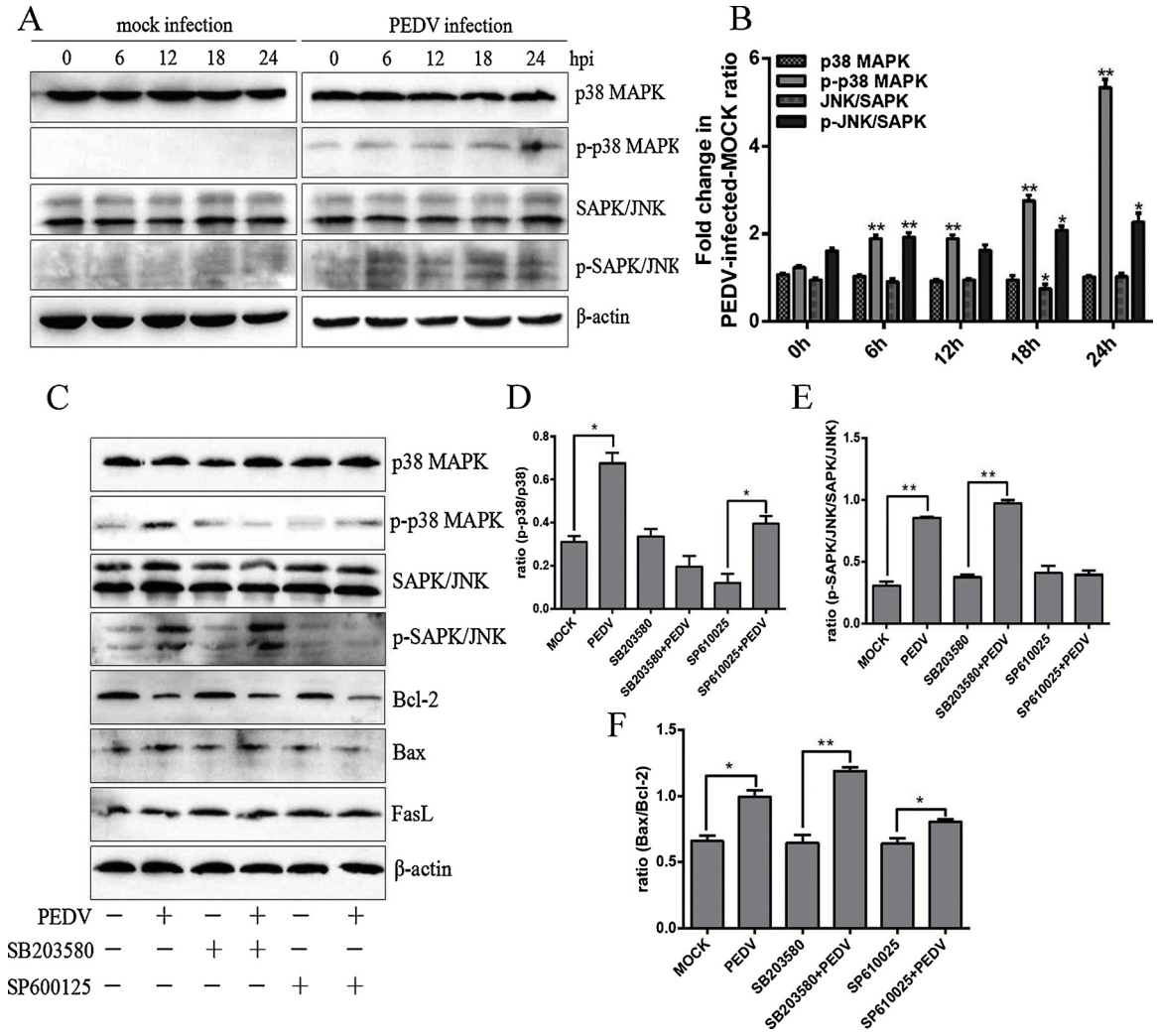

Fig. 8. The activation of p38-MAPK signalling by PEDV infection and its effect on apoptosis. A. Vero cells were mock or PEDV infected for different time periods. Western blot analysis was performed using the indicated antibodies to detect phosphorylated p38 and JNK. B. Representative densitometries of phosphorylated p38 and JNK were calculated after being normalised to β-actin using Image J. C. Western blot analysis was performed to detect p38 MAPK, p-p38 MAPK, SAPK/JNK, p-SAPK/JNK, Bax, Bcl-2 and FasL in the presence or absence of SB203580 and SP600125. D. The ratio of p-p38 MAPK/p38 MAPK was analysed and presented as a histogram. E. The ratio of p-SAPK/JNK was analyzed and presented as a histogram. F. The ratio of Bax/Bcl-2 was analysed and presented as a histogram. Results are representative of three independent experiments. Data are represented as mean ± SD, n = 3. (*, $p < 0.05$; **, $p < 0.01$).

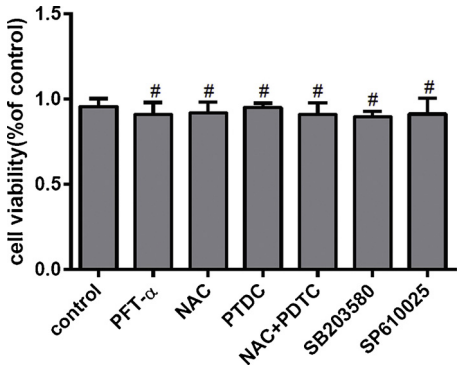

Fig. 9. The effect of molecular inhibitors on cell activity measured by MTT assay. Cells were grown on 96-well plates and incubated with inhibitors or antioxidants at different concentrations (10 μM PFT-α, 10 μM SB203580, 10 μM SP600125, 5 mM NAC and 50 μM PDTC) for 24 h and MTT assays were performed. Results are representative of three independent experiments. Data are represented as mean ± SD, n = 3. (*,$p < 0.05$; **, $p < 0.01$;#, no significant difference).

during PEDV infection, however, treatment with an excessive amount of inhibitors may have adverse effects on cell activity and cause cytotoxicity that disturbs normal cell metabolism. Similar examples can be found in rafoxanide against MM cells (Xiao et al., 2019), PFOS against SH-SY5Y cells (Li et al., 2015) and plumbagin against MCF-7 (A), SK-OV-3 (B), and MCF-10A (De et al., 2019). Thus, to exclude the effect of inhibitors on the toxicity of cells, we tested the inhibitory effect of cells in the presence of inhibitor and antioxidant treatment for 24 h. Results showed that treatment with 10 μM PFT-α, 10 μM SB203580, 10 μM SP600125, 5 mM NAC and 50 μM PDTC had no inhibitory effect on cell viability, which indicated that there was no significant influence in cells treated with inhibitor and antioxidant for 24 h. Therefore, the influence of signalling inhibitors on cells can be excluded, in other words, all changes in those proteins tested were caused by PEDV.

Collectively, our data provide a link between ROS, p53 and apoptosis induced by PEDV infection. The results demonstrate that PEDV infection induced apoptosis in Vero cells via activated p53 signalling and ROS accumulation. Our findings may provide insights into the mechanism of PEDV interaction with p53 and ROS, and help to reveal the pathogenesis of PEDV infection. A schematic diagram depicting the signalling pathways required for PEDV activation and PEDV-induced

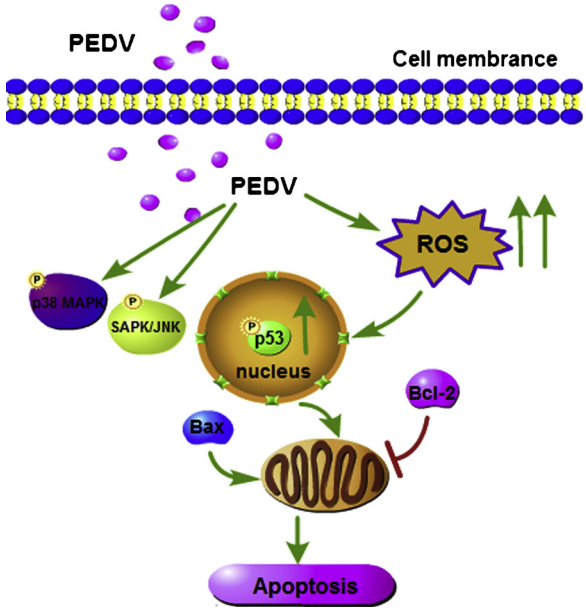

Fig. 10. Schematic diagram of the PEDV-induced apoptosis signalling pathway. PEDV infection increased ROS accumulation and further promoted p53 activation and transfer of p53 to the nucleus. PEDV infection promoted apoptosis by increasing Bax expression and inhibiting Bcl-2 expression. Inhibition of activated p53 and ROS reduced the ratio of Bax/Bcl-2 and apoptotic rate, thus ROS and p53 participated in PEDV-induced apoptosis. PEDV infection activated p38 MAPK and SAPK/JNK signal pathway whereas p38 MAPK and SAPK/JNK activation had nothing to do with PEDV-induced apoptosis. →: activation; ⊥: inhibition.

apoptosis is shown in Fig. 10. Further studies on the mechanisms of PEDV-induced apoptosis should provide new insights into the interplay between PEDV and its host.

Competing interests

The authors declare that they have no competing interests.

Authors' contributions

Xingang Xu and Ying Xu performed the majority of the experiments and were involved in preparation of the manuscript. Qi Zhang and Feng Yang participated in the editing of the manuscript. Zheng Yin and Lixiang Wang participated in the experimental work. Qinfan Li conceived the study, participated in its design and coordination, and revised the manuscript. All authors have read and approved the final manuscript.

Acknowledgement

This work was supported by grants from the Special Fund for Agro-scientific Research of Shaanxi Province (No. 20180711000005), the Science and Technology Planning Project of Yangling Agricultural High-tech Demonstration Area (No. 2018NY-10), and the Science and Technology Project of Xian City (No. 2017050NC/NY010), China.

References

Bálint, é., Vousden, K.H., 2001. Activation and activities of the p53 tumour suppressor protein. Br. J. Cancer 85 (12), 1813–1823.
Bao, F.K., 1996. The bcl-2 gene family, an important regulator of apoptosis. Sheng li ke xue jin zhan [Progress Physiol.] 27 (1), 67–69.
Barber, N.G., 2001. Host defense, viruses and apoptosis. Cell Death Differ. 8 (2), 113–126.
Bragado, P., Armesilla, A., Silva, A., Porras, A., 2007. Apoptosis by cisplatin requires p53 mediated p38α MAPK activation through ROS generation. Apoptosis 12 (9), 1733–1742.
Carpio, M.A., Michaud, M., Zhou, W., Fisher, J.K., Walensky, L.D., Katz, S.G., 2015. BCL-2 family member BOK promotes apoptosis in response to endoplasmic reticulum stress [Cell Biology]. Proc. Natl. Acad. Sci. U. S. A. 112 (23), 7201–7206.
Chen, C.J., Sugiyama, K., Kubo, H., Huang, C., Makino, S., 2004. Murine coronavirus nonstructural protein p28 arrests cell cycle in G0/G1 phase. J. Virol. 78 (19), 10410–10419.
Chen, S., Cheng, A.C., Wang, M.S., Peng, X., 2008. Detection of apoptosis induced by new type gosling viral enteritis virus in vitro through fluo-rescein annexin V-FITC/PI double labeling. World J. Gastroenterol. 14 (14), 2174–2178.
Chen, Y., Zhang, Z., Li, J., Gao, Y., Zhou, L., Ge, X., Han, J., Guo, X., Yang, H., 2018. Porcine epidemic diarrhea virus S1 protein is the critical inducer of apoptosis. Virol. J. 15 (1), 170.
Circu, M.L., Aw, T.Y., 2010. Reactive oxygen species, cellular redox systems, and apoptosis. Free Radic. Biol. Med. 48 (6), 749–762.
Cory, S., Huang, D.C.S., Adams, J.M., 2003. The Bcl-2 family: roles in cell survival and oncogenesis. Oncogene 22 (53), 8590–8607.
Dabiri, Y., Schmid, A., Theobald, J., Blagojevic, B., Streciwilk, W., Ott, I., Wölfl, S., Cheng, X., 2018. A ruthenium(II) N-Heterocyclic carbene (NHC) complex with naphthalimide ligand triggers apoptosis in colorectal Cancer cells via activating the ROS-p38 MAPK pathway. Int. J. Mol. Sci. 19 (12), E3964.
De, U., Son, J.Y., Jeon, Y., Ha, S.Y., Park, Y.J., Yoon, S., Ha, K.T., Choi, W.S., Lee, B.M., Kim, I.S., Kwak, J.H., Kim, H.S., 2019. Plumbagin from a tropical pitcher plant (Nepenthes alata Blanco) induces apoptotic cell death via a p53-dependent pathway in MCF-7 human breast cancer cells. Food Chem. Toxicol. 123, 492–500.
Egberink, H.F., Ederveen, J., Callebaut, P., Horzinek, M.C., 1988. Characterization of the structural proteins of porcine epizootic diarrhea virus, strain CV777. Am. J. Vet. Res. 49 (8), 1320–1324.
Elmore, S., 2007. Apoptosis: a review of programmed cell death. Toxicol. Pathol. 35 (4), 495–516.
Fuh, K.C., Meneshian, A., Patel, C.B., Takiar, V., Bulkley, G.B., 2002. Signal transduction by reactive oxygen species: alternative paradigms for signaling specificity. Surgery 131 (6), 601–612.
Gallenne, T., Gautier, F., Oliver, L., Hervouet, E., Noël, B., Hickman, J.A., Geneste, O., Cartron, P.F., Vallette, F.M., Manon, S., Juin, P., 2009. Bax activation by the BH3-only protein Puma promotes cell dependence on antiapoptotic Bcl-2 family members. J. Cell Biol. 185 (2), 279–290.
Gao, M., Monian, P., Pan, Q., Zhang, W., Xiang, J., Jiang, X., 2016. Ferroptosis is an autophagic cell death process. Cell Res. 26 (9), 1021–1032.
Gary, L., Johnson, R.L., 2002. Mitogen-activated protein kinase pathways mediated by ERK, JNK, and p38 protein kinases. Science 298 (5600), 1911–1912.
Hamanaka, R.B., Chandel, N.S., 2010. Mitochondrial reactive oxygen species regulate cellular signaling and dictate biological outcomes. Trends Biochem. Sci. 35 (9), 505–513.
Hao, W., Wang, S., Zhou, Z., 2015. Tubeimoside-1 (TBMS1) inhibits lung cancer cell growth and induces cells apoptosis through activation of MAPK-JNK pathway. Int. J. Clin. Exp. Pathol. 8 (10), 12075–12083.
Hristov, G., Melanie, Krämer, Li, J., El-Andaloussi, N., Mora, R., Daeffler, L., Zentgraf, H., Rommelaere, J., Marchini, A., 2010. Through its nonstructural protein NS1, parvovirus H-1 induces apoptosis via accumulation of reactive oxygen species. J. Virol. 84 (12), 5909–5922.
Huang, Y., Ding, L., Li, Z., Dai, M., Zhao, X., Li, W., Du, Q., Xu, X., Tong, D., 2013. Transmissible gastroenteritis virus infection induces cell apoptosis via activation of p53 signalling. J. Gen. Virol. 94 (Pt 8), 1807–1817.
Kastenhuber, E.R., Lowe, S.W., 2017. Putting p53 in context. Cell 170 (6), 1062–1078.
Kim, Y., Lee, C., 2014. Porcine epidemic diarrhea virus induces caspase-independent apoptosis through activation of mitochondrial apoptosis-inducing factor. Virology 460–461, 180–193.
Kusanagi, K., Kuwahara, H., Katoh, T., Nunoya, T., Ishikawa, Y., Samejima, T., Tajima, M., 1992. Isolation and serial propagation of porcine epidemic diarrhea virus in cell cultures and partial characterization of the isolate. J. Vet. Med. Sci. 54 (2), 313–318.
Lan, H., Yuan, H., Lin, C., 2017. Sulforaphane induces p53-deficient SW480 cell apoptosis via the ROS-MAPK signaling pathway. Mol. Med. Rep. 16 (5), 7796–7804.
Laptenko, O., Prives, C., 2006. Transcriptional regulation by p53: one protein, many possibilities. Cell Death Differ. 13 (6), 951–961.
Lee, C., Kim, Y., Jeon, J.H., 2016. JNK and p38 mitogen-activated protein kinase pathways contribute to porcine epidemic diarrhea virus infection. Virus Res. 222, 1–12.
Li, W., He, Q.Z., Wu, C.Q., Pan, X.Y., Wang, J., Tan, Y., Shan, X.Y., Zeng, H.C., 2015. PFOS disturbs BDNF-ERK-CREB signaling in association with increased microRNA-22 in SH-SY5Y Cells. Biomed Res. Int. 2015, 302653.
Miyata, Y., Matsuo, T., Sagara, Y., Ohba, K., Ohyama, K., Sakai, H., 2017. A mini-review of reactive oxygen species in urological Cancer: correlation with NADPH oxidases, angiogenesis, and apoptosis. Int. J. Mol. Sci. 18 (10), E2214.
Mizutani, T., Fukushi, S., Saijo, M., Kurane, I., Morikawa, S., 2004. Phosphorylation of p38 MAPK and its downstream targets in SARS coronavirus-infected cells. Biochem. Biophys. Res. Commun. 319 (4), 1228–1234.
Nazim, U.M., Park, S.Y., 2018. Attenuation of autophagy flux by 6-shogaol sensitizes human liver cancer cells to TRAIL-induced apoptosis via p53 and ROS. Int. J. Mol. Med. 43 (2), 701–708.
Reed, L.J., 1938. A simple method of estimating fifty percent endpoints. Am. J. Epidemiol. 27, 493–497.
Shang, Y.Y., Yao, M., Zhou, Z.W., Cui, J., Li, X., Hu, R.Y., Yu, Y.Y., Gao, Q., Yang, B., Liu, Y.X., Dang, J., Zhou, S.F., Yu, N., 2017. Alisertib promotes apoptosis and autophagy in melanoma through p38 MAPK-mediated aurora a signaling. Oncotarget 8 (63), 107076–107088.
Stevenson, G.W., Hoang, H., Schwartz, K.J., Burrough, E.R., Sun, D., Madson, D., Cooper,

V.L., Pillatzki, A., Gauger, P., Schmitt, B.J., Koster, L.G., Killian, M.L., Yoon, K.J., 2013. Emergence of Porcine epidemic diarrhea virus in the United States: clinical signs, lesions, and viral genomic sequences. J. Vet. Diagn. Invest. 25 (5), 649–654.
Sun, D., Wang, X., Wei, S., Chen, J., Feng, L., 2016. Epidemiology and vaccine of porcine epidemic diarrhea virus in China: a mini-review. J. Vet. Med. Sci. 78 (3), 355–363.
Sun, P., Wu, H., Huang, J., Xu, Y., Yang, F., Zhang, Q., Xu, X., 2018. Porcine epidemic diarrhea virus through p53-dependent pathway causes cell cycle arrest in the G0/G1 phase. Virus Res. 253, 1–11.
Tang, L., Wu, Y., 2016. Bcl-2 family proteins regulate apoptosis and epithelial to mesenchymal transition by calcium signals. Curr. Pharm. Des. 22 (30), 4700–4704.
Torres, M.A., Jones, J.D., Dang, J.L., 2006. Reactive oxygen species signaling in response to pathogens. Plant Physiol. 141 (2), 373–378.
Tung, W.H., Tsai, H.W., Lee, I.T., Hsieh, H.L., Chen, W.J., Chen, Y.L., Yang, C.M., 2010. Japanese encephalitis virus induces matrix metalloproteinase-9 in rat brain astrocytes via NF-κB signaling dependent on MAPKs and reactive oxygen species. Br. J. Pharmacol. 161 (7), 1566–1583.
Xiao, W., Xu, Z., Chang, S., Li, B., Yu, D., Wu, H., Xie, Y., Wang, Y., Xie, B., Sun, X., Kong, Y., Lan, X., Bu, W., Chen, G., Gao, L., Wu, X., Shi, J., Zhu, W., 2019. Rafoxanide, an organohalogen drug, triggers apoptosis and cell cycle arrest in multiple myelomaby enhancing DNA damage responses and suppressing the p38 MAPK pathway. Cancer Lett. 444, 45–59.
Xu, J., Zhang, S., 2015. Mitogen-activated protein kinase cascades in signaling plant growth and development. Trends Plant Sci. 20 (1), 56–64.
Yan, Y., Du, Y., Wang, G., Deng, Y., Li, R., Li, K., 2016. The novel H7N9 influenza a virus NS1 induces p53-Mediated apoptosis of A549 cells. Cell. Physiol. Biochem. 38 (4), 1447–1458.
Yang, D.K., Kim, H.H., Lee, S.H., Yoon, S.S., Park, J.W., Cho, I.S., 2018. Isolation and characterization of a new porcine epidemic diarrhea virus variant that occurred in Korea in 2014. J. Vet. Sci. 19 (1), 71–78.
Zhang, H., Huang, Y., Du, Q., Luo, X., Zhang, L., Zhao, X., Tong, D., 2015. Porcine parvovirus infection induces apoptosis in PK-15 cells through activation of p53 and mitochondria-mediated pathway. Biochem. Biophys. Res. Commun. 456 (2), 649–655.
Zhao, S., Gao, J., Zhu, L., Yang, Q., 2014. Transmissible gastroenteritis virus and porcine epidemic diarrhoea virus infection induces dramatic changes in the tight junctions and microfilaments of polarized IPEC-J2 cells. Virus Res. 192, 34–45.
Zhao, X., Xiang, H., Bai, X., Fei, N., Huang, Y., Song, X., Zhang, H., Zhang, L., Tong, D., 2016. Porcine parvovirus infection activates mitochondria-mediated apoptotic signaling pathway by inducing ROS accumulation. Virol. J. 13 (1), 26.
Zheng, H., Xu, L., Liu, Y., Li, C., Zhang, L., Wang, T., Zhao, D., Xu, X., Zhang, Y., 2018. MicroRNA-221-5p inhibits porcine epidemic diarrhea virus replication by targeting genomic viral RNA and activating the NF-κB pathway. Int. J. Mol. Sci. 19 (11), E3381.
Zhou, P., Tu, L., Lin, X., Hao, X., Zheng, Q., Zeng, W., Zhang, X., Zheng, Y., Wang, L., Li, S., 2017. Cfa-miR-143 promotes apoptosis via the p53 pathway in canine influenza virus H3N2-Infected cells. Viruses 9 (12), E360.